Stereoisomerism and Ring-Chain Tautomerism in 1-Hydroxy-2,3-dihydro-1*H*-pyrazolo[1,2-*a*]pyridazine-5,8-diones and 1-Hydroxy- and 1-Amino-2,3-dihydro-1*H*-pyrazolo[1,2-*b*]phthalazine-5,10-diones

Jari Sinkkonen,*[a] Vladimir Ovcharenko,[a] Kirill N. Zelenin,[b] Irina P. Bezhan,[b] Boris A. Chakchir,[c] Fatema Al-Assar,[c] and Kalevi Pihlaja[a]

Keywords: Heterocycles / NMR spectroscopy / Structure elucidation / Tautomerism

1-Hydroxy-2,3-dihydro-1*H*-pyrazolo[1,2-*a*]pyridazine-5,8-diones and 1-hydroxy- and 1-amino-2,3-dihydro-1*H*-pyrazolo[1,2-*b*]phthalazine-5,10-diones were synthesized and their structures studied by NMR and MS methods. All compounds exist in similar cyclic forms in solution, except for 1-hydroxy-1-methyl-2,3-dihydro-1*H*-pyrazolo[1,2-*a*]pyridazine-5,8-dione, which displays ring-chain tautomerism in $CDCl_3$ solution. The corresponding 3-methyl-substituted derivatives exhibit a typical *cis*/*trans* isomerism as a result of latent ring-chain-ring tautomerism. The structures of stereoisomers concluded from NMR results were additionally confirmed by density functional calculations. Mass spectrometric results indicate open-chain structures in the gas phase for the molecular ions of the 1-hydroxy derivatives and cyclic structures for 1-amino derivatives.

Introduction

1,2-Disubstituted hydrazides react with α,β-unsaturated carbonyl compounds to afford hydroxypyrazolidines. Their chemical properties[1] and pharmacological activity[2] have been systematically investigated. The same reaction also takes place with hydrazides of dicarboxylic acids,[3,4] although the available information on the product structures is not comprehensive.[3−8] From IR and UV spectra the condensation products were reported[4,5] to have linear structures. The NMR results,[3,6] which are more convincing, suggest that cyclic hydrazides react with acrolein and crotonaldehyde by forming condensed pyrazolidines, whereas methyl vinyl ketone gives open-chain products. The literature data do not deal comprehensively with *cis*/*trans* isomerism in the case of pyrazolidine derivatives obtained from crotonaldehyde or with the existence of ring-chain tautomerism in these systems. In order to fill these gaps, we have studied in detail the structures of the previously known condensation products **Ia−e**[3−6] (Scheme 1), derived from maleic and phthalic hydrazides, and of their novel analogues **IIIa−e** (Scheme 2), synthesized by reactions between derivative **Ie** and the corresponding amines **II**.

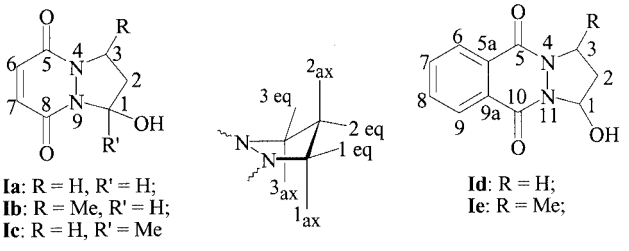

Ia: R = H, R' = H;
Ib: R = Me, R' = H;
Ic: R = H, R' = Me

Id: R = H;
Ie: R = Me;

Scheme 1. Structures of compounds **Ia−e**, including the numbering system and the naming of the protons in the pyrazolo moiety

Determination of their solution structures was carried out by ^1H and ^{13}C NMR spectroscopy in [D_6]DMSO and $CDCl_3$ as solvents. In addition, theoretical calculations were made for selected compounds to confirm the stereochemical conclusions inferred from the NMR results. Gas-phase structures were also examined by mass spectrometric methods. The use of a variety of modern methods offers wider insight into the possibly existing isomeric structures of molecules.

Results and Discussion

NMR Results

NMR measurements were made in two solvents: [D_6]DMSO and $CDCl_3$. The proton spectra were first measured as soon as possible after the compound has dissolved (usually within 10 minutes). The spectra were taken again

[a] Structural Chemistry Group, Department of Chemistry, University of Turku,
Vatselankatu 2, 20014 Turku, Finland
Fax: (internat.) +358−2/3336700
E-mail: jari.sinkkonen@utu.fi
[b] Russian Military Medical Academy,
194044 Saint Petersburg, Russia
[c] Saint Petersburg Chemico-Pharmaceutical Academy,
193376 Saint Petersburg, Russia

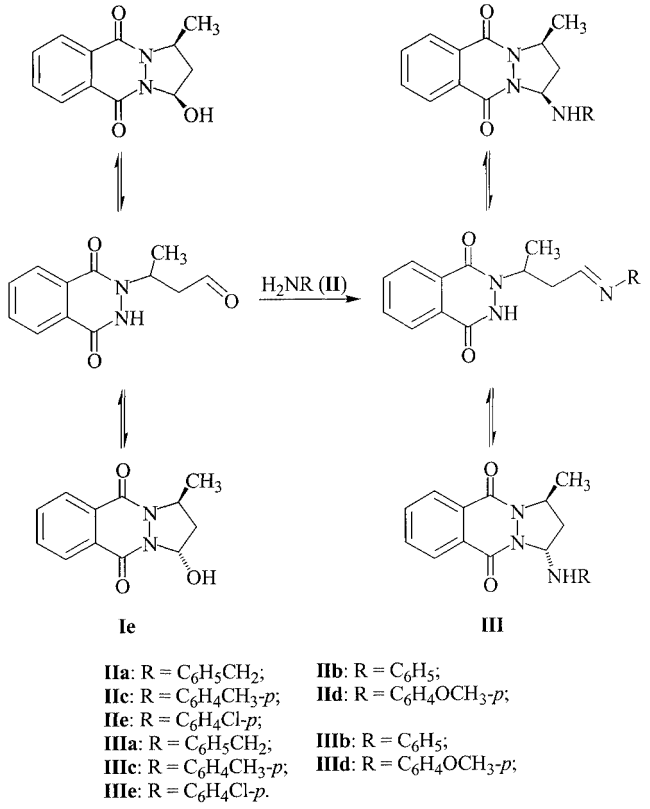

Scheme 2. Synthesis and structures of compounds **IIIa−e**

after one day and also after some weeks. The ^{1}H and ^{13}C chemical shifts and the H,H coupling constants in [D$_6$]DMSO are presented in Tables 1 and 2. The values of the coupling constants for compounds **I** were obtained by using PERCH simulation and iteration software.[9]

Compounds **Ia** and **Id** existed entirely in cyclic forms in both solvents and no time dependence was observed in their spectra. For compounds **Ib** and **Ie**, two cyclic forms were observed. For both compounds and in both solvents, the ratio between the forms was very close to 3:1 and did not change over time. This suggests that an equilibrium mixture of the *cis* and *trans* isomers had already been formed during the synthesis. The cyclic forms were deduced to be *cis* and *trans* isomers with respect to the pyrazolidine ring substituents, the *cis* isomers being identified from the values of the vicinal coupling constants of protons in the 2-positions (Table 1). Since only very small vicinal couplings were observed for one of these protons [2$_{eq}$-H, see Scheme 1 for (pseudo)equatorial and (pseudo)axial protons], the torsion angles between protons 2$_{eq}$-H and 1-H and also between protons 2$_{eq}$-H and 3-H must be close to 90° (Karplus-like dependence[10]), which is geometrically possible only if both substituents are on the same side of the ring. This fact is confirmed by geometry calculations (vide infra). The proton chemical shifts for 2$_{eq}$-H and 2$_{ax}$-H also show a clear difference between the *cis* and *trans* isomers. For the *cis* forms they are approx. δ = 1.8 and 2.5 ppm,

Table 1. Relative amounts of the isomers, selected ^{1}H and ^{13}C chemical shifts, and ^{1}H,^{1}H coupling constants for compounds **Ia−e** recorded at 30 °C in [D$_6$]DMSO (referenced internally to the solvent signals with values δ = 2.49 ppm for ^{1}H and δ = 39.50 ppm for ^{13}C); chemical shifts are in ppm and coupling constants in Hz; values of the coupling constants were obtained (excluding **Ic**) from PERCH simulation and by use of iteration software[9]

	Ia	**Ib** (*cis*)	**Ib** (*trans*)	**Ic**	**Id**	**Ie** (*cis*)	**Ie** (*trans*)
Ratio (%)	100	76	24	100	100	77	23
1-H/1-Me	5.98	5.96	5.96	2.10	6.15	6.13	6.11
1-OH	7.10	7.20	7.05	–	7.08	7.16	7.03
2$_{eq}$-H	2.04	1.82	2.27	2.81	2.11	1.88	2.34
2$_{ax}$-H	2.31	2.49	2.07	(2$_{ax}$ = 2$_{eq}$)	2.38	2.56	2.13
3$_{eq}$-H/3-Me$_{eq}$	4.18	4.61	1.43	4.03	4.34	4.77	1.51
3$_{ax}$-H/3-Me$_{ax}$	3.88	1.43	4.55	(3$_{ax}$ = 3$_{eq}$)	4.01	1.52	4.69
C-1	80.45	80.32	79.29	206.57	80.28	80.20	79.03
C-2	30.02	36.35	38.49	1.10	30.37	36.66	38.88
C-3	44.83	54.49	54.90	5.32	44.73	54.31	54.62
C-1-Me	–	–	–	9.86	–	–	–
C-3-Me	–	19.13	18.24	–	–	19.44	18.67
J(1,1-OH)	5.8	4.7	5.9	–	3.7	4.6	5.8
J(1,2$_{eq}$)	0.6	0.2	1.8	–	1.7	0.3	1.3
J(1,2$_{ax}$)	5.4	6.0	5.9	–	5.1	5.9	5.5
J(2$_{eq}$,2$_{ax}$)	−13.0	−13.2	−13.3	–	−12.9	−13.1	−13.2
J(2$_{eq}$,3$_{eq}$)	1.3	0.7	–	7.2	1.4	0.4	–
J(2$_{eq}$,3$_{ax}$)	7.0	–	8.5	–	6.9	–	8.5
J(2$_{ax}$,3$_{eq}$)	9.3	8.9	–	–	9.2	8.9	–
J(2$_{ax}$,3$_{ax}$)	11.3	–	7.3	–	11.3	–	7.3
J(3$_{eq}$,3$_{ax}$)	−11.8	–	–	–	−11.5	–	–
J(3$_{eq}$,3-Me)	–	6.6	–	–	–	6.5	–
J(3$_{ax}$,3-Me)	–	–	6.2	–	–	–	6.2

Table 2. Relative amounts of the isomers, ^{1}H and ^{13}C chemical shifts and selected ^{1}H,^{1}H coupling constants for compounds **IIIa−e** recorded at 30 °C in [D_6]DMSO (referenced internally to the solvent signals using values δ = 2.49 ppm for ^{1}H and δ = 39.50 ppm for ^{13}C); chemical shifts are in ppm and coupling constants in Hz

	IIIa (*cis*)	**IIIa** (*trans*)	**IIIb** (*cis*)	**IIIb** (*trans*)	**IIIc** (*cis*)	**IIIc** (*trans*)	**IIId** (*cis*)	**IIId** (*trans*)	**IIIe** (*cis*)	**IIIe** (*trans*)
DMSO (%)	44	56	44	56	45	55	42	58	42	58
$CDCl_3$ (%)	40	60	50	50	50	50	48	52	57	43
1-H	5.58	5.76	6.06	6.26	6.02	6.21	5.99	6.16	6.03	6.27
2_{eq}-H	2.00	2.45	2.02	2.46	2.01	2.45	2.02	2.45	2.01	2.44
2_{ax}-H	2.65	2.17	2.76	2.31	2.75	2.29	2.75	2.29	2.78	2.31
3-H	4.71	4.81	4.81	4.85	4.80	4.84	4.80	4.84	4.81	4.84
3-Me	1.61	1.45	1.59	1.54	1.58	1.53	1.59	1.53	1.57	1.53
H-NH	3.29	3.60	6.39	6.53	6.17	6.34	5.95	6.16	6.59	6.72
H-*ortho*	7.37	7.25	6.76	6.84	6.69	6.75	6.77	6.82	6.81	6.87
H-*meta*	7.27	7.17	7.13	7.09	6.94	6.89	6.77	6.71	7.16	7.11
H-*para*	7.18	7.06	6.64	6.60	–	–	–	–	–	–
H-*others*	3.94, 4.00	3.74, 3.80	–	–	2.17	2.13	3.66	3.63	–	–
C-1	72.70	72.40	67.85	67.03	68.23	67.45	69.00	68.27	67.88	67.11
C-2	34.76	35.43	35.37	37.59	35.36	37.53	35.41	37.46	35.33	37.49
C-3	54.59	54.08	54.51	54.36	54.52	54.35	54.54	54.37	54.42	54.20
C-3-Me	20.01	18.53	19.71	18.66	19.73	18.37	19.77	18.38	19.67	18.32
C-*ipso*	140.63	140.31	146.18	145.93	143.91	143.53	140.30	139.70	145.17	145.04
C-*ortho*	127.75	127.50	112.87	113.29	113.13	113.58	114.56	115.09	114.39	114.79
C-*meta*	127.99	127.86	128.86	128.63	129.26	129.10	114.46	114.28	128.51	128.32
C-*para*	126.44	126.32	116.93	117.15	125.46	125.69	151.70	151.81	120.44	120.55
C-*others*	50.02	47.57	–	–	20.04	20.01	55.26	55.19	–	–
$J(1,2_{eq})$	<1	3.3	<1	2.3	<1	2.3	<1	1.8	<1	3.0
$J(1,2_{ax})$	7.7	7.0	6.8	6.7	6.5	6.9	6.5	*n.r.*[a]	6.8	6.8
$J(2_{eq},2_{ax})$	−13.0	−12.9	−13.0	−12.9	−13.0	−12.8	−12.9	−12.7	−13.0	−13.0
$J(2_{eq},3)$	<1	7.7	<1	7.1	<1	7.0	<1	7.0	<1	7.4
$J(2_{ax},3)$	7.9	7.2	9.2	8.3	9.2	8.2	8.9	*n.r.*	9.1	7.7
J(3,3-Me)	6.4	6.2	6.7	6.0	6.6	6.0	6.7	6.2	6.7	6.2
J(1,NH)	*n.r.*	*n.r.*	5.9	8.6	5.8	8.5	5.6	*n.r.*	5.9	8.9

[a] *n.r.* not resolved.

whereas for the *trans* forms the shifts are much closer to each other (2.1 and 2.3 ppm). This is easy to understand, since the magnetic environment of 2_{eq}-H in the *cis* isomer differs greatly from that of 2_{ax}-H (both substituents are on the same side of the ring). Godin and Le Berre also observed proton signals for two forms, but were not able to identify the isomers.[3] Nakamura and Kamiya later published more detailed ^{1}H NMR results, including the values of coupling constants,[6] which were in better agreement with our stereochemical conclusions.

Compound **Ic** exists in the linear form in [D_6]DMSO. This can be seen from, for example, the presence of carbonyl carbon at δ = 206.57 ppm (Table 1). The solubility of **Ic** in $CDCl_3$ was very low and hence only the proton spectrum was measurable. Two forms, linear and cyclic, were identified in $CDCl_3$. The proton signals for the cyclic form were found at δ = 2.38 and 2.49 ppm (2_{eq}-H and 2_{ax}-H), δ = 3.90 and 4.26 ppm (3_{eq}-H and 3_{ax}-H), and δ = 1.89 ppm (1-Me). The ratio between the linear and the cyclic forms was approx. 4:1. This is the first case in which ring-chain tautomerism has been observed for this compound. A few drops of [D_6]DMSO or trifluoroacetic acid made the sample more soluble, but no cyclic form was then observed. The reason for this is most probably that DMSO is capable of dissolving the linear form of the molecule so well as to make the small amount of the cyclic form, which is soluble in $CDCl_3$, negligible in the spectra. The compound's solubility in [D_6]acetone or [D_4]methanol was even poorer than in $CDCl_3$. The earlier studies on this compound suggest a linear form. Two C=O bands were observed in the infrared spectrum:[5] one for ring carbonyls and one for the carbonyl group in the side chain. The old (low resolution) NMR results[3] for this compound suggested the linear form on the basis of the large difference in the chemical shifts of 6-H and 7-H.

Signals for two cyclic forms are found in the NMR spectra of compounds **IIIa−e**, and were assigned to *cis* and *trans* isomers with respect with the substituents on the five-membered ring, similarly to the hydroxy derivatives. The ^{1}H and ^{13}C chemical shifts and selected ^{1}H,^{1}H coupling constants for compounds **IIIa−e** are given in Table 2. Some general remarks can be made on the chemical shifts of compounds **IIIa−e**. The chemical shift of the methyl carbon in each case is at least 1 ppm larger for *cis* isomers than for *trans* isomers. The same trend can also be seen in the methyl proton shifts. The 2-H proton chemical shifts are also clearly different for the *cis* and *trans* isomers, as in the hydroxy derivatives. The shifts for the 2-H protons in the *cis* forms are δ = approx. 2.0 and 2.7 ppm, while in the *trans* forms they are much closer to each other (δ = approx. 2.3 and 2.45 ppm).

Measurements were made also in $CDCl_3$, and the relative amounts of the *cis* and *trans* isomers are listed in Table 2. In conclusion, the *trans* isomer is usually somewhat favored,

especially in [D_6]DMSO, but not very much. The time dependencies of the *cis*/*trans* ratios were also studied. In compounds **IIIa–d,** no changes were observed, but in compound **IIIe** the relative amounts immediately after dissolution were *cis*/*trans* = 83:17 (in [D_6]DMSO) and 93:7 (in $CDCl_3$). Thus, the chlorine-substituted compound appears to be the only case in which the equilibrium is not achieved immediately. The presence of the time and solvent dependence, unlike in compounds **I**, also suggests the existence of ring-linear-ring tautomerism in these systems, since the transformation of the *cis* and *trans* forms into one another occurs through the linear intermediate (Scheme 2). The contribution of the linear form, however, is not large enough to be seen in the spectra.

MS Results

The EI mass spectra of all studied compounds (**I** and **III**) are shown in Table 3. The EI mass spectra of compounds **I** show abundant $M^{+\cdot}$ ion peaks (Table 4), which seem to show that the compounds exist predominantly as open-chain isomers (*N*-substituted cyclic hydrazides). The base peaks in all cases (except **Ic**) correspond either to a_1 (Scheme 3) or to $[a_1 - N_2H_2]^{+\cdot}$ ions (in the maleic hydrazide derivatives **Ia-b**). The direct formation of a_1 ions from $M^{+\cdot}$ (as confirmed by metastable transitions) points to the open-chain forms. The loss of the side chain from open-chain $M^{+\cdot}$ isomers, producing a_1 ions, is readily explained by assuming a six-centered, McLafferty-type rearrangement. On the other hand, formation of a_1 ions from cyclic $M^{+\cdot}$ ions would require consecutive cleavages of two C–N bonds, accompanied by two H transfers from the leaving fragment. Similarly, $[M - C_2H_3O]^+$ ions (a_2 in Scheme 3) can be produced directly from open-chain $M^{+\cdot}$ by a single-bond cleavage. It should be noted that the only ketone derivative in this series, **Ic** (R′ = Me), produces exceptionally abundant $[M - C_2H_3O]^+$ ions (Table 4).

Table 3. EI (70 eV) mass spectra of compounds **I** and **III** (fragment peaks of > 5% RA are listed)

Compound	*m/z* (% RA)
Ia	168(M, 55) 151(6) 125(7) 113(6) 112(72) 98(9) 82(100) 80(8) 58(6) 57(25) 55(14) 54(45) 53(6)
Ib	183(8) 182(M, 77) 165(7) 154(10) 139(19) 113(28) 112(94) 98(9) 82(100) 71(18) 70(9) 69(9) 57(63) 55(15) 54(41) 53(8)
Ic	182(M, 39) 164(15) 140(11) 139(100) 125(22) 113(19) 112(87) 98(32) 83(7) 82(57) 80(32) 71(17) 70(10) 58(9) 55(35) 54(18)
Id	219(10) 218 (M, 72) 201(7) 190(26) 175(20) 163(10) 162(100) 148(20) 132(10) 130(22) 105(11) 104(58) 77(6) 76(33) 75(5) 50(9)
Ie	233(9) 232(M, 65) 189(29) 163(16) 162(100) 148(18) 132(7) 130(21) 105(17) 104(50) 77(8) 76(38) 75(7) 50(13)
IIIa	321(M, 4) 216(5) 162(24) 161(12) 160(91) 159(21) 144(15) 132(10) 130(6) 106(25) 105(5) 104(20) 92(14) 91(100) 77(5) 76(8) 65(8)
IIIb	307(M, 16) 216(14) 215(100) 146(31) 145(7) 144(7) 130(11) 104(9) 77(9) 76(5)
IIIc	321(M, 21) 216(14) 215(100) 199(5) 162(8) 160(27) 159(19) 158(14) 144(9) 130(9) 107(8) 104(9) 91(9) 76(5)
IIId	337(M, 34) 216(14) 215(100) 176(22) 175(66) 174(17) 173(5) 162(30) 160(34) 134(6) 132(8) 130(11) 123(17) 115(5) 105(6) 104(17) 77(9) 76(6)
IIIe	343(M, 3) 341(M, 9) 216(14) 215(100) 180(10) 179(10) 178(7) 162(11) 144(5) 130(11) 111(5) 104(8) 76(5)

Table 4. Characteristic ions in the 70 eV EI mass spectra of compounds **Ia–e** (% of the total ion current; TIC); see Scheme 3 for ion compositions

Compd.	$M^{+\cdot}$	a_1	$a_1 - N_2H_2$	$a_2 = [M - C_2H_3O]$	*b*	$b - H_2O$
Ia	10.8	12.9	17.9	1.3	1.6	1.4
Ib	12.1	13.2	14.0	2.7	1.3	1.0
Ic	6.6	12.7	8.6	3.2[a]	4.7	4.6
Id	16.6	20.1	1.9	4.0	3.9	4.4
Ie	12.9	17.5	1.3	5.1	3.1	3.6

[a] For this compound only, $a_2 = [M - C_3H_5O]^+$, and $[M - C_2H_3O]^+$ is the base peak (14.6% TIC).

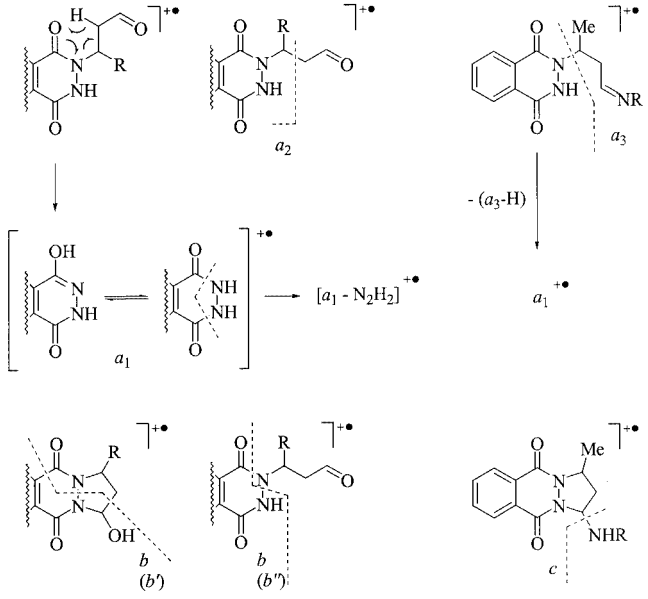

Scheme 3. Main fragmentation routes of compounds **I** and **III** under EI

None of the significant fragment ions observed in the spectra of **Ia–e** can safely be assigned to cyclic $M^{+\cdot}$ isomers. An interesting fragmentation process is the formation of *b*, or $[M - RC_3H_3NO]^+$ ions (Scheme 3), directly from $M^{+\cdot}$. These *b* ions were shown to decompose further by loss of a water molecule. Regardless of the $M^{+\cdot}$ structure, *b* ions cannot be formed by any simple mechanism involving a single bond cleavage. Moreover, Scheme 3 demonstrates that the neutral leaving fragment, RC_3H_3NO, may include either one of the ring carbonyls (if $M^{+\cdot}$ is assumed to have a cyclic structure) or, conversely, the side- chain carbonyl

(if the fragmentation is initiated from an open-chain $M^{+\cdot}$ structure and accompanied by a hydrogen transfer), giving rise to the isobaric structures *b′* and *b″*, respectively. Any conceivable cyclic $M^{+\cdot}$ structure fragmentation mechanism giving rise to *b″* ions with intact carbonyl oxygens would have to involve two H transfers from the leaving group, which is hardly compatible with the direct formation of *b* ions from the $M^{+\cdot}$. Experiments with ^{18}O-labelled starting compounds could have provided the decisive evidence as to whether the *b* ions originated from cyclic or open-chain $M^{+\cdot}$ structures of **I**. In the absence of such evidence, however, *b* and [*b* − H_2O] ions cannot be unequivocally assigned to cyclic $M^{+\cdot}$ forms.

In spite of the structural similarity between compounds **I** and **III**, the mass spectra of the latter are dominated by $[M - NHR]^+$ ion peaks (Table 5), which strongly points to the cyclic structure for $M^{+\cdot}$. Another significant difference, brought about by the introduction of arylamino moieties, is in the positive charge distribution during the loss of the side chain from open-chain $M^{+\cdot}$ isomers of **I** and **III**. In the case of compounds **I**, the side chain is always lost as a neutral fragment, giving a_1 ions. In the case of compounds **III**, the charge is preferably localized in the side chain, so that a_3 ions are more abundant than a_1 ions (Scheme 3) except in the case of **IIId** (in this compound, R = 4-$MeOC_6H_4$, the electron-donating nature of the aromatic substituent reverses the a_1/a_3 ratio.)

Table 5. Characteristic ions in the 70 eV EI mass spectra of compounds **IIIa−e** (% of the total ion current; TIC); see Scheme 3 for ion compositions

Compd.	$M^{+\cdot}$	a_1	$(M - a_1) = (a_3 - H)$	a_3^+	$c^+ = (M - RNH)$	R^+
IIIa	1.2	5.2	4.5	19.8	1.0	21.7
IIIb	6.6	1.3	2.3	10.9	34.8	3.0
IIIc	7.6	2.2	5.5	7.8	29.1	2.7
IIId	7.8	5.7	12.5	4.1	19.0	0.5
IIIe	4.5	3.3	4.5	4.0	31.6	2.0

Analysis of the mass spectra of compounds **I** and **III** shows the absence of any direct correlation between the preferred isomeric structures in solution and in the gas phase. Although the amino derivatives **III** are structurally similar to the parent compounds **I**, and $M^{+\cdot}$ ions of **I** and **III** share a number of fragmentation patterns (such as the formation of a_1 ions), their EI mass spectra cannot be directly compared or correlated with the respective structures of neutral compounds as observed in solution by NMR methods. No peaks of $[M - OH]^+$ or $[M - H_2O]^{+\cdot}$ ions (analogous to $[M - NHR]^+$ ions in **III**) were observed in the mass spectra of **I**, so no direct comparison of the cyclic/linear ratios of $M^{+\cdot}$ isomers on the basis of the relative abundances of a_1 (a_3) and *c* ions is possible.

Calculations

Theoretical calculations were performed for the cyclic isomers of compounds **Ia** and **Ib**. The main purpose was to confirm the molecular geometry inferred from the observed $^1H,^1H$ coupling constants from NMR spectroscopic data. Calculations for compounds **Id** and **Ie** were not needed, because they showed behavior very similar to that of their pyridazine analogues. In addition, these results can be qualitatively applied to the conformations of compounds **III**.

The geometry optimizations were made for the structures in two major envelope-shaped pyrazolo ring conformations, in which the off-plane carbon can flip and convert the (pseudo)axial and (pseudo)equatorial protons/substituents (Scheme 1) into one another. These conformations are named as in Figure 1, and so **Ia** has two conformations (OH_{ax} and OH_{eq}) depending on whether the OH is axial or equatorial and **Ib** has two *cis* ($OH_{ax}Me_{ax}$ and $OH_{eq}Me_{eq}$) and two *trans* conformations ($OH_{ax}Me_{eq}$ and $OH_{eq}Me_{ax}$). The initial structures were constructed by molecular mechanics methods and the final optimizations were performed by the density functional theoretic method B3LYP/6-31G (d,p) with Gaussian 98[11] software. The optimized structures are shown in Figure 1 and the torsion angles for the pyrazolo moiety and the energies of the structures are presented in Table 6.

By comparing the values of the observed coupling constants (Table 1) with the values of the calculated torsion angles it is easily seen that, to produce a small coupling constant between the protons in positions 1 and 2, the protons must both be equatorial (torsion angle close to 90 degrees). This indicates that the OH group in the observed conformations is always axial, and the conformations determined from the spectroscopic data are thus OH_{ax} for **Ia**, $OH_{ax}Me_{ax}$ for **Ib**-*cis*, and $OH_{ax}Me_{eq}$ for **Ib**-*trans*. The conformations OH_{ax} for **Ia** and $OH_{ax}Me_{ax}$ for **Ib**-*cis* are also in agreement with the small observed coupling constants between the protons 2_{eq} and 3_{eq}. The values of the energies, however, are not in agreement with the observed results. For compound **Ia** the calculation predicts OH_{eq} to have the minimum energy, although by a small amount. For compound **Ib**, calculation predicts the correct structure for the *cis* isomer but the wrong one for the *trans* isomer. Actually, the calculations clearly favor axial methyl group whereas the observed results show a strong tendency towards structures with axial hydroxyl groups, ignoring the effect of the methyl substituents. It might be that interactions between the carbonyl oxygen and the hydroxyl proton (i.e., hydrogen bonding) stabilize the axial OH group.

Calculations for gas-phase structures at 0 K were made first. Because the relative energies did not fit to observations, additional calculations taking account of the DMSO solvent were performed. These calculations were made by the PCM method (DMSO, at 298 K) with Gaussian 98[11] software. The results from these calculations (Table 6) had no significant consequences for the relative stabilities of the conformers. The same is also valid with the results from SCI-PCM calculations performed for the conformations of the *trans* isomers.

Although the energy values from calculations were not in agreement with the observed results, the optimization geometries (i.e., the values of the torsion angles) can be used

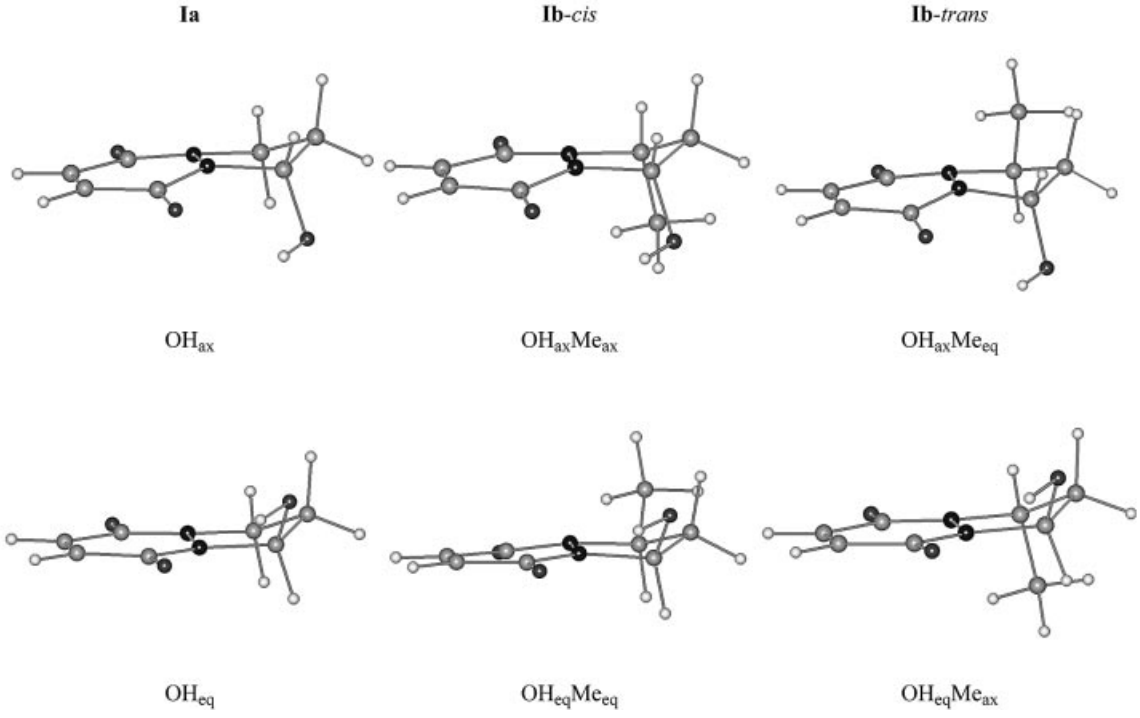

Figure 1. Structures of the main conformations of **Ia** and **Ib** optimized by the B3LYP/6-31G (d,p) method

Table 6. Torsion angles and energy values for the main conformations (see Figure 1) of the compounds **Ia** and **Ib** calculated by the B3LYP/6-31G (d,p) method

	OH_{ax} **Ia**	OH_{eq} **Ia**	$OH_{ax}Me_{ax}$ **Ib** (*cis*)	$OH_{eq}Me_{eq}$ **Ib** (*cis*)	$OH_{ax}Me_{eq}$ **Ib** (*trans*)	$OH_{eq}Me_{ax}$ **Ib** (*trans*)
$\tau(1_{eq},2_{eq})$	95.9	–	96.6	–	96.4	–
$\tau(1_{eq},2_{ax})$	−23.8	–	−22.9	–	−23.3	–
$\tau(1_{ax},2_{eq})$	–	−31.6	–	−31.7	–	−30.7
$\tau(1_{ax},2_{ax})$	–	−150.9	–	−150.8	–	−149.7
$\tau(2_{eq},3_{eq})$	−93.1	−90.6	−97.1	–	–	−95.5
$\tau(2_{eq},3_{ax})$	30.8	33.2	–	34.0	32.5	–
$\tau(2_{ax},3_{eq})$	29.1	31.6	24.7	–	–	26.3
$\tau(2_{ax},3_{ax})$	156.0	155.4	–	155.0	153.5	–
E/Hartree[a]	−606.722267	−606.722682	−646.043648	−646.042422	−646.042280	−646.043203
ΔE/kJ mol^{-1} [b]	+1.1	0	0	+3.2	+3.6	+1.2
E^S/Hartree[c]	−606.732408	−606.732774	−646.053011	−646.051535	−646.051314	−646.052711
ΔE^S/kJ mol^{-1}[b,c]	+0.96	0	0	+3.9	+4.5	+0.79

[a] Energy for gas phase structures at 0 K. [b] Energy relative to the lowest energy structure of **Ia** and **Ib**. [c] Energy for which the solvent (DMSO) was taken into account by PCM method at 298 K.

qualitatively to identify the conformations not only for compounds **Ia** and **Ib** but also for **Id**, **Ie**, and for the whole set of new compounds **III**, which display behavior very similar to that of compound **Ib** as far as the values of the coupling constants are concerned.

Conclusion

A set of previously known 1-hydroxy-2,3-dihydro-1*H*-pyrazolo[1,2-*a*]pyridazine-5,8-diones and pyrazolo[1,2-*b*]-phthalazine-5,10-diones (**I**, Scheme 1) and novel 1-amino-2,3-dihydro-1*H*-pyrazolo[1,2-*b*]phthalazine-5,10-diones (**III**, Scheme 2) were synthesized and their structures studied by NMR and mass spectrometric methods, supported by theoretical calculations. Compounds **I** (except for **Ic**) have cyclic structures, and *cis*/*trans* isomerism was observed when 3-methyl substituents were present (in **Ib** and **Id**). The *cis* and *trans* isomers were identified by the values of the $^1H,^1H$ coupling constants in the pyrazolo moieties, and the assignments were confirmed by the values of the torsion angles obtained from molecular modeling results. The ring-chain tautomerism observed for the first time in compound **Ic** in $CDCl_3$ provides an explanation for the existence of *cis*/*trans* equilibria in the pyrazolidine derivatives **I**, which are likely to involve open-chain forms at concentrations so low as to preclude their detection by NMR techniques. Compounds **III** existed as cyclic *cis* and *trans* isomers. The

identification of the forms was easy with the aid of the coupling constant values for **I**.

In contradiction to the similarities observed in the NMR spectra of compounds **I** and **III**, the mass spectra show a clear difference between them. The molecular ions $M^{+\cdot}$ of compounds **I** (except for **Ic**) exist as open-chain forms, unlike the molecules in solution. For the amino derivatives **III**, however, the molecular ions relate strongly to the cyclic structures. These results represent a demonstration of different behavior in the gas phase (mass spectrometry) and in solution (NMR).

Experimental Section

NMR Measurements: NMR spectra were acquired on a JEOL JNM-A-500 spectrometer operating at 500.16 MHz for ^{1}H and 125.78 MHz for ^{13}C or a JEOL JNM-L-400 spectrometer operating at 399.78 MHz for ^{1}H and 100.54 MHz for ^{13}C. Spectra were recorded at 30 °C for samples in [D_6]DMSO and at 25 °C for samples in $CDCl_3$. Proton and carbon spectra were referenced internally to solvent signals, using values of δ = 2.49 ppm for proton (middle peak) and δ = 39.50 ppm for carbon (middle peak) in [D_6]DMSO and δ = 7.26 ppm for proton and δ = 77.00 ppm for carbon (middle peak) in $CDCl_3$. One-dimensional proton spectra were acquired with normal single-pulse excitation, 45° flip angle, and with spectral widths of 7 kHz consisting of 32 K data points. One-dimensional carbon spectra were acquired with normal single-pulse excitation, broad-band proton decoupling, 45° flip angle, and with spectral widths of 30 kHz consisting of 65 K data points and with 0.3−0.5 Hz exponential weighting applied prior to Fourier transformation. DEPT spectra (135°) were acquired and processed under similar conditions. Two-dimensional heteronuclear one-bond correlation experiments were acquired either by carbon-detected CH-shift correlation with partial homonuclear decoupling in the f1 dimension or by proton-detected HMQC with gradient selection. Long-range heteronuclear correlation experiments included either carbon-detected COLOC or proton-detected HMBC with gradient selection. The one-bond coupling constant was 145 Hz and the long-range coupling constants were 5−12 Hz in proton-carbon correlation spectra. Two-dimensional homonuclear H,H-correlation experiments were acquired by phase-sensitive double quantum filtered COSY. The spectral widths of two-dimensional spectra were optimized from one-dimensional spectra. All spectra were produced by using standard pulse sequences. The proton spectra were analyzed by PERCH simulation and with iteration software.[9]

MS Measurements: The electron-impact mass spectra were recorded on a VG ZabSpec mass spectrometer (Manchester, UK) at 70 eV (direct insertion probe, ion source temperature 160 °C). Elemental compositions of fragment ions were determined from accurate mass measurements at a resolution of 10 000−12 000 (10% valley definition) by the peak matching technique, with perfluorokerosene (PFK) as a reference compound. Metastable ion spectra (B/E and B^2/E linked scan technique, decompositions in the 1FFR) were recorded with the same instrument. All the fragmentation processes discussed in the text are confirmed by metastable ion spectra.

Calculations: The results of molecular mechanics optimizations were used as starting points for density functional calculations based on unrestricted Becke's three-parameter hybrid[12] involving the gradient-corrected correlation functional of Lee, Yang, and Parr[13] (B3LYP) and using the standard 6-31G (d,p) basis set. These calculations were made with the Gaussian 98 package.[11] Solvent effect calculations were performed by using the polarized continuum (overlapping spheres) model (PCM[14−16]) or the self-consistent isodensity PCM (SCI-PCM[17]) model at the same level of theory as the geometry optimizations above. These calculations were also performed with Gaussian 98.[11]

Synthesis of Compounds Ia−e

Method A (for Ia, Ib, and Ie):[1] Maleic or phthalic hydrazides (0.1 mol) were heated with the corresponding carbonyl compounds (0.7 mol) in a sealed metallic container at 150 °C (oil bath) for 3−5 h (maleic hydrazide) or 7 h (phthalic hydrazide). The unchanged carbonyl compound was removed under reduced pressure, and the residue was recrystallized from ethyl acetate or ethanol.

Method B (for Ic and Id):[2] Aqueous NaOH (20%, 3 drops) was added to a slurry of hydrazide (0.05 mol) and carbonyl compound (0.07 mol) in 50 mL of ethanol, and the reaction mixture was heated under reflux for 12 h (**Ic**) or 2 days (**Id**). The unchanged hydrazide was filtered off, and the precipitate formed upon cooling was recrystallized from ethanol.

1-Hydroxy-2,3-dihydro-1*H*-pyrazolo[1,2-*a*]pyridazine-5,8-dione (Ia): Yield: 57% (9.58 g). M.p. 179−178 °C[1] (ethyl acetate). $C_7H_8N_2O_3$ (168.15) calcd. (%): C 50.00, H 4.80, N 16.66; found (%): C 50.18, H 4.69, N 16.51. NMR spectroscopic data are listed in Table 1, additional data ([D_6]DMSO, ppm): δ = 6.90, 6.94 (6-H, 7-H), 152.96, 153.46 (C-5, C-8), 135.33, 135.89 (C-6, C-7). MS data in Tables 3 and 4.

1-Hydroxy-3-methyl-2,3-dihydro-1*H*-pyrazolo[1,2-*a*]pyridazine-5,8-dione (Ib): Yield: 71% (12.93 g). M.p. 161−162 °C[1] (ethanol). $C_8H_{10}N_2O_3$ (182.18) calcd. (%): C 52.74, H 5.53, N 15.38; found (%): C 52.88, H 5.65, N 15.49. NMR spectroscopic data in Table 1, additional data ([D_6]DMSO, ppm): 6.92, 6.92 (6-H, 7-H, *cis*), 152.58, 153.32 (C-5, C-8, *cis*), 135.33, 136.35 (C-6, C-7, *cis*), 6.92, 6.92 (6-H, 7-H, *trans*), 153.74, 154.07 (C-5, C-8, *trans*), 135.27, 136.85 (C-6, C-7, *trans*) ppm. MS data in Tables 3 and 4.

1-Hydroxy-1-methyl-2,3-dihydro-1*H*-pyrazolo[1,2-*a*]pyridazine-5,8-dione (Ic): Yield: 51% (4.65 g). M.p. 149 °C[3] (ethanol). $C_8H_{10}N_2O_3$ (182.18) calcd. (%): C 52.74, H 5.53, N 15.38; found (%): C 52.95, H 5.71, N 15.21. NMR spectroscopic data in Table 1, additional data ([D_6]DMSO), ppm): 6.85, 7.01 (6-H, 7-H), 152.56, 157.87 (C-5, C-8), 126.96, 132.72 (C-6, C-7). MS data in Tables 3 and 4.

1-Hydroxy-2,3-dihydro-1*H*-pyrazolo[1,2-*b*]phthalazine-5,8-dione (Id): Yield: 75% (8.18 g). M.p. 212−213 °C[1] (ethanol). $C_{11}H_{10}N_2O_3$ (218.21) calcd. (%): C 60.55, H 4.62, N 12.84; found (%): C 60.48, H 4.71, N 12.73. NMR spectroscopic data in Table 1, additional data ([D_6]DMSO, ppm): 8.15, 8.15 (6-H, 9-H), 7.87, 7.87 (7-H, 8-H), 153.24, 153.74 (C-5, C-10), 129.54, 129.75 (C-5a, C-9a) 126.53, 126.80 (C-6, C-9), 133.07, 133.45 (C-7, C-8). MS data in Tables 3 and 4.

1-Hydroxy-3-methyl-2,3-dihydro-1*H*-pyrazolo[1,2-*b*]phthalazine-5,8-dione (Ie): Yield: 77% (17.88 g). M.p. 151−152 °C[1] (ethanol). $C_{12}H_{12}N_2O_3$ (232.24) calcd. (%): C 62.06, H 5.21, N 12.06; found (%): C 61.91, H 5.15, N 12.20. NMR spectroscopic data in Table 1, additional data ([D_6]DMSO), ppm): 8.15, 8.17 (6-H, 9-H, *cis*), 7.86, 7.89 (7-H, 8-H, *cis*), 152.81, 153.49 (C-5, C-10, *cis*), 129.53, 130.00 (C-5a, C-9a, *cis*) 126.56, 126.73 (C-6, C-9, *cis*), 133.06, 133.42 (C-7, C-8, *cis*), 8.15, 8.17 (6-H, 9-H, *trans*), 7.86, 7.89 (7-H, 8-H, *trans*), 153.95, 154.31 (C-5, C-10, *trans*), 129.58, 130.35 (C-5a, C-9a, *trans*) 126.56, 126.73 (C-6, C-9, *trans*), 133.10, 133.49 (C-7, C-8, *trans*). MS data in Tables 3 and 4.

Synthesis of Compounds III: A mixture of **Ia−b** (10 mmol) and amine **II** (10 mmol) was heated under reflux in 10 mL of benzene. The reaction was monitored by TLC. After completion of the reaction, the solvent was removed under reduced pressure, the residue was washed with diethyl ether, and the product was recrystallized from benzene (**III**). The chemical shifts of the phthalazine-5,10-dione moiety are not given either in Table 2 or separately after each compound, because the shifts were very similar in all compounds and in both forms. For all compounds they are 8.10−8.21 ppm (6-H, 9-H); 7.81−7.92 ppm (7-H, 8-H); 152.8−154.6 ppm (C-5, C-10); 129.5−130.4 ppm (C-5a, C-9a); 126.3−126.8 ppm (C-6, C-9); 132.8−133.6 ppm (C-7, C-8).

1-(Benzylamino)-3-methyl-2,3-dihydro-1*H*-pyrazolo[1,2-*b*]phthalazine-5,10-dione (IIIa): Yield: 43% (1.38 g). M.p. 105−107 °C (benzene). R_f = 0.89 (in chloroform/methanol 10:0.3). $C_{19}H_{19}N_3O_2$ (321.37) calcd. (%): C 71.01, H 5.96, N 13.08; found (%): C 70.84, H 6.12, N 12.85. NMR spectroscopic data in Table 2 and MS data in Tables 3 and 5.

1-Anilino-3-methyl-2,3-dihydro-1*H*-pyrazolo[1,2-*b*]phthalazine-5,10-dione (IIIb): Yield: 53% (1.63 g). M.p. 148−149 °C (benzene). R_f = 0.58 (in chloroform/methanol 10:0.3). $C_{18}H_{17}N_3O_2$ (307.35) calcd. (%): C 70.34, H 5.57, N 13.67; found (%): C 70.19, H 5.48, N 13.78. NMR spectroscopic data in Table 2 and MS data in Tables 3 and 5.

3-Methyl-1-[(4-methylphenyl)amino]-2,3-dihydro-1*H*-pyrazolo[1,2-*b*]phthalazine-5,10-dione (IIIc): Yield: 96% (3.09 g). M.p. 95−96 °C (benzene). R_f = 0.58 (in chloroform/methanol 10:0.3). $C_{19}H_{19}N_3O_2$ (321.37) calcd. (%): C 71.01, H 5.96, N 13.08; found (%): C 70.89, H 6.07, N 13.21. NMR spectroscopic data in Table 2 and MS data in Tables 3 and 5.

1-[(4-Methoxyphenyl)amino]-3-methyl-2,3-dihydro-1*H*-pyrazolo[1,2-*b*]phthalazine-5,10-dione (IIId): Yield: 92% (3.10 g). M.p. 98−100 °C (benzene). R_f = 0.70 (in chloroform/methanol 10:0.3). $C_{19}H_{19}N_3O_3$ (337.37) calcd. (%): C 67.64, H 5.68, N 12.45; found (%): C 67.81, H 5.72, N 12.31. NMR spectroscopic data in Table 2 and MS data in Table 3 and 5.

1-[(4-Chlorophenyl)amino]-3-methyl-2,3-dihydro-1*H*-pyrazolo[1,2-*b*]phthalazine-5,10-dione (IIIe): Yield: 92% (3.11 g). M.p. 180−182 °C (benzene). R_f = 0.57 (in chloroform/methanol 10:0.3). $C_{18}H_{16}ClN_3O_2$ (341.79) calcd. (%): C 63.25, H 4.72, N 12.29; found (%): C 63.14, H 4.61, N 12.12. NMR spectroscopic data in Table 2 and MS data in Tables 3 and 5.

Acknowledgments

The authors wish to thank the Academy of Finland for financial support.

[1] K. N. Zelenin, *Org. Prep. Proc. Int.* **1995**, *27*, 519−540.
[2] K. N. Zelenin, I. P. Bezhan, L. V. Pastushenkov, E. G. Gromova, E. E. Lesiovskaja, B. A. Chakchir, L. F. Melnikova, *Arzneimittel Forschung Drug Research* **1999**, *49(II)*, 10, 843−848.
[3] J. Godin, A. Le Berre, *Bull. Soc. Chim. Fr.* **1968**, *10*, 4229−4234.
[4] S. Kamiya, A. Nakamura, *Chem. Pharm. Bull.* **1967**, *15*, 949−958; *Chem. Abstr.* **1968**, *68*, 29993.
[5] H. Feuer, R. Harmetz, *J. Am. Chem. Soc.* **1958**, *5*, 5877−5880.
[6] A. Nakamura, S. Kamiya, *Yakugaku Zasshi* **1970**, *90*, 1069−1075.
[7] A. Csámpai, K. Körmendy, F. Ruff, *Tetrahedron* **1991**, *45*, 4457−4464.
[8] F. J. Weigert, *J. Org. Chem.* **1978**, *43*, 622−626.
[9] See for example, R. Laatikainen, M. Niemitz, U. Weber, J. Sundelin, T. Hassinen, J. Vepsäläinen, *J. Magn. Reson. Ser. A* **1996**, *120*, 1, or the program website at: http://www.uku.fi/perch.html.
[10] M. Karplus, *J. Chem. Phys.* **1959**, *30*, 11−15.
[11] M. J. Frisch, G. W. Trucks, H. B. Schlegel, G. E. Scuseria, M. A. Robb, J. R. Cheeseman, V. G. Zakrzewski, J. A. Montgomery, Jr., R. E. Stratmann, J. C. Burant, S. Dapprich, J. M. Millam, A. D. Daniels, K. N. Kudin, M. C. Strain, O. Farkas, J. Tomasi, V. Barone, M. Cossi, R. Cammi, B. Mennucci, C. Pomelli, C. Adamo, S. Clifford, J. Ochterski, G. A. Petersson, P. Y. Ayala, Q. Cui, K. Morokuma, P. Salvador, J. J. Dannenberg, D. K. Malick, A. D. Rabuck, K. Raghavachari, J. B. Foresman, J. Cioslowski, J. V. Ortiz, A. G. Baboul, B. B. Stefanov, G. Liu, A. Liashenko, P. Piskorz, I. Komaromi, R. Gomperts, R. L. Martin, D. J. Fox, T. Keith, M. A. Al-Laham, C. Y. Peng, A. Nanayakkara, M. Challacombe, P. M. W. Gill, B. Johnson, W. Chen, M. W. Wong, J. L. Andres, C. Gonzalez, M. Head-Gordon, E. S. Replogle, J. A. Pople, *Gaussian 98*, revision A.11; Gaussian, Inc.: Pittsburgh, PA, **2001**.
[12] A. D. Becke, *J. Chem. Phys.* **1993**, *98*, 5648−5652.
[13] C. Lee, W. Yang, R. G. Parr, *Phys. Rev. B* **1988**, *37*, 785−789.
[14] S. Miertus, E. Scrocco, J. Tomasi, *Chem. Phys.* **1981**, *55*, 117−129.
[15] S. Miertus, J. Tomasi, *Chem. Phys.* **1982**, *65*, 239−245.
[16] M. Cossi, V. Barone, R. Cammi, J. Tomasi, *Chem. Phys. Lett.* **1996**, *255*, 327−335.
[17] J. B. Foresman, T. A. Keith, K. B. Wiberg, J. Snoonian, M. J. Frisch, *J. Phys. Chem.* **1996**, *100*, 16098−16104.

Received February 5, 2002
[O02069]